

## A global quantum Monte Carlo approach for the persistent current in an Aharonov - Bohm ring with interacting electrons

This article has been downloaded from IOPscience. Please scroll down to see the full text article.

1996 J. Phys.: Condens. Matter 8 L413

(<http://iopscience.iop.org/0953-8984/8/30/001>)

View [the table of contents for this issue](#), or go to the [journal homepage](#) for more

Download details:

IP Address: 171.66.16.206

The article was downloaded on 13/05/2010 at 18:21

Please note that [terms and conditions apply](#).

LETTER TO THE EDITOR

# A global quantum Monte Carlo approach for the persistent current in an Aharonov–Bohm ring with interacting electrons

Qianghua Wang<sup>†‡</sup>, Jian-Xin Zhu<sup>‡</sup> and Z D Wang<sup>‡</sup>

<sup>†</sup> Department of Physics, Nanjing University, Nanjing 210093, People's Republic of China

<sup>‡</sup> Department of Physics, University of Hong Kong, Pokfulam, Hong Kong

Received 6 February 1996, in final form 30 May 1996

**Abstract.** We propose a quantum Monte Carlo approach for the study of the thermo-equilibrium persistent current in an Aharonov–Bohm ring with interacting electrons. From topological considerations we derive a formula for the current, which leads to a global quantum Monte Carlo algorithm to evaluate the global current–phase relation at a given temperature without going into simulations point-by-point in the phase. Notable features in the present approach are: (i) the problem of complex elements in the representation of the partition function is well-handled, (ii) being robust against possible randomness in the Hamiltonian, the basic formula captures all phase-dependent physics and hence makes the simulation itself extremely efficient and reliable.

As was once mentioned by Hirsch [1], there are almost as many different quantum Monte Carlo techniques as there are problems one wants to solve. Numerical simulation of the many-fermion problem is difficult because of the anti-commutating rule for the fermion fields. In particular, to the best of our knowledge, an efficient quantum Monte Carlo method that would simulate the problem in which complex transfer matrix elements are relevant is not yet available. In this letter we concerned ourselves with the thermo-equilibrium persistent current in an Aharonov–Bohm ring, where the above-mentioned problem does appear and will be solved in a unique way. We study this system because of its importance in its own right. With the fabrication of smaller and smaller samples and the routine availability of low temperatures, new physics mainly due to the quantum phase-coherent effects has emerged from the studies of small devices. In particular, since the seminal work of Büttiker *et al* [2], there has been much theoretical [3–7] and experimental [8] interest in the persistent current in mesoscopic rings which enclose an Aharonov–Bohm [9] flux:  $\Phi = \oint \mathbf{A} \cdot d\mathbf{l}$  where  $\mathbf{A}$  is the vector potential. Recently, the numerical calculations with interactions included in the Hamiltonian were performed by the exact diagonalization technique [10], the Hartree–Fock approximation [11], and the Bethe ansatz solution [7]. These methods are limited to quantum mechanical calculation and are difficult to generalize to include the effect of finite temperatures. Cheung *et al* [3] have studied analytically the finite temperature behaviour of a model ring with free electrons. However, when the interaction is present such a study is difficult or even impossible. We propose here for the first time a novel quantum Monte Carlo approach for the study of the persistent current, which may provide rich information on the roles played by various parameters, such as the temperature, inhomogeneity and nature of the Coulomb interaction in a unified manner.

Such investigations have long been desirable in order to distinguish between different origins of the experimental results.

Our approach is closest in spirit to a general quantum Monte Carlo method for fermions developed by Hirsch, Scalapino and Sugar (HSS) [12]. The distinguishing advantage of our approach is that the basic formula we derived captures all phase dependence in the partition function and thus makes the simulation procedure itself extremely practical and efficient: the *global* current–phase characteristics at a given temperature can be obtained from a single round of simulations, *without going into simulations point-by-point in the phase*. Our method is based on the consideration of topology and may thus be applicable to a large amount of topologically equivalent systems in condensed matter physics other than the mesoscopic ring considered here.

To simplify the presentation, we begin with the model Hamiltonian for  $M$  spinless fermions in a one-dimensional ring of  $N$  lattice sites in a magnetic field:

$$H = \sum_i \epsilon_i n_i - t \left[ \sum_i e^{i\theta} C_i^\dagger C_{i+1} + \text{h.c.} \right] + V \sum_i \left( n_i - \frac{1}{2} \right) \left( n_{i+1} - \frac{1}{2} \right) \quad (1)$$

where  $n_i = C_i^\dagger C_i$ ,  $C_i^\dagger$  and  $C_i$  are the usual fermion creation and annihilation operators in the Wannier state at the  $i$ th lattice site and  $\epsilon_i$  is the on-site energy, which can be either uniform or random from  $i$  to  $i'$ . Here  $t > 0$  is the hopping matrix element, and  $\theta = \varphi/N = 2\pi\Phi/N\Phi_0$  where  $\Phi$  is the magnetic flux threading the ring and  $\Phi_0 = h/e$  is the flux quantum. Finally  $V$  is a measure of the short-range (nearest neighbour) Coulomb interaction between the fermions. We shall limit ourselves in the case of the spinless fermions described by equation (1) as far as the Monte Carlo method is concerned. The possibility to include the spin-degrees of freedom and randomness in the hopping matrix element  $t$  and the local phase  $\theta$  (with the total phase  $\varphi$  unchanged) will be discussed in the following development.

From the Trotter formula the partition function for  $M$  fermions at a temperature  $T$  can be written as [12, 13],

$$Z_M = \text{Tr}_M e^{-\beta H} \approx \text{Tr}_M (U_1 U_2)^L = \sum_{i_1, i_2, \dots, i_{2L}} \langle i_1 | U_1 | i_2 \rangle \langle i_2 | U_2 | i_3 \rangle \cdots \langle i_{2L} | U_2 | i_1 \rangle \quad (2)$$

where  $U_1 = e^{-\Delta\tau H_1}$ ,  $U_2 = e^{-\Delta\tau H_2}$  with  $\Delta\tau = \beta/L$  and  $\beta = 1/k_B T$ , and a complete set of states (in the lattice-occupation representation) at each time slice are inserted. Here the total Hamiltonian has been broken up as the sum of  $H_1$  and  $H_2$ , each of which is composed of sums of pieces that commute piece-wise between themselves. In particular, for the Hamiltonian given in equation (1), the decomposition can be made as  $H = H_1 + H_2 = \sum_{\text{odd } i} H_{i,i+1} + \sum_{\text{even } i} H_{i,i+1}$  with

$$H_{i,i+1} = -(t e^{i\theta} C_i^\dagger C_{i+1} + \text{h.c.}) + V \left( n_i - \frac{1}{2} \right) \left( n_{i+1} - \frac{1}{2} \right) + \frac{1}{2} (\epsilon_i n_i + \epsilon_{i+1} n_{i+1}). \quad (3)$$

The error in equation (2) is of order  $(\Delta\tau)^2$  [12]. The evaluation of the matrix elements in equation (2) reduces to solving a two-site problem. A graphical representation of the element in equation (2) for a 4-site ring with two fermions is the checkerboard lattice shown in figure 1 (see also [12, 13]). The shaded regions indicate sites which are connected by the time evolution operator. Each element in equation (2) is a product of all of the sub-elements represented by the shaded boxes on the checkerboard. The sum over intermediate states in equation (2) can be performed by importance sampling if the elements are real and non-negative. For convenience, world lines can be drawn for each fermion as in figure 1. As pointed out in [12], since  $H_{i,i+1}$  conserves fermion number locally in a shaded box, a world

line can only be moved at a given time interval if it is running along a vertical edge of a shaded box. In that case it can be moved across the adjacent unshaded box. The Boltzmann factor for such a move depends only on the occupation states of the four shaded boxes connecting that unshaded box. It is important to note that due to the local conservation law for the fermion number, world-lines never move diagonally in an unshaded box. The efficiency of the above updating rule is the major advantage of the HSS algorithm.

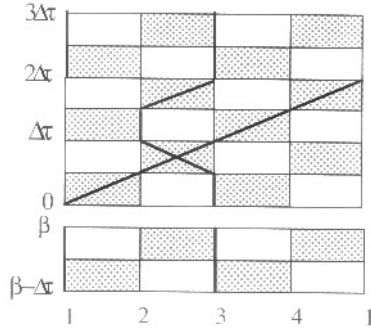


**Figure 1.** A checkerboard lattice (not completely shown) for a 4-site ring with  $M = 2$  fermions. The horizontal direction is the spatial direction, and the vertical direction is the imaginary time (Trotter) direction. World-lines for the fermions are shown by the bold lines.

Being slightly different from the definition given in [12], we find it convenient to define the winding number of an allowed configuration in the following manner. First we assign a ‘charge’ number  $n_s = 0$  to a shaded box with no fermions, or with fermions moving forward, and a ‘charge’ number  $n_s = +1$  ( $n_s = -1$ ) to a shaded box with a fermion moving north-west (north-east) (see figure 1 for guidance). Note that a shaded box with two fermions crossing each other is equivalent to that with two fermions moving forward. Then the winding number  $n$  is simply evaluated as  $n = \sum_s n_s / N$  where the summation is over the shaded boxes on the whole checkerboard. Due to the cyclic boundary condition in the imaginary-time (or Trotter) and the spatial directions, it is found that the allowed values of  $n$  are  $n = 0, \pm 1, \pm 2, \dots$ , and that  $n$  is conserved during the updating process described above. Therefore each  $n$  identifies a specific topology of the configuration. All of the configurations with the same  $n$  form a subspace of the total space spanned by all of the *allowed* configurations. Furthermore, the total ‘charge’ in each column of the checkerboard in our case is identically  $n$ . These findings will simplify the following derivation considerably.

It can be seen that in our case, the elements in equation (2) are complex in general (although the complete summation is indeed real). A direct sampling from the partition function  $Z_M$  becomes invalid. Instead, one must use an auxiliary partition function

$$\tilde{Z}_M = \sum_{i_1, i_2, \dots, i_{2L}} |\langle i_1 | U_1 | i_2 \rangle \langle i_2 | U_2 | i_3 \rangle \cdots \langle i_{2L} | U_2 | i_1 \rangle| \quad (4)$$

where the modulus operation is applied for each element. A remarkable feature of  $\tilde{Z}_M$  is its independence of  $\theta$  (or  $\varphi$ ), as we shall show immediately. By solving the two-site problem, we find that to an element in  $Z_M$  (being a product of all the sub-elements represented by the shaded boxes), a shaded box involving the operator  $e^{-\Delta\tau H_{i,i+1}}$  with ‘charge’  $n_s$  contributes a sub-element  $e^{i n_s [\theta + (M-1)\pi \delta_{i,N}]} \Gamma_s$  where  $\delta_{i,N}$  is the usual Kronecker delta function,  $\Gamma_s$  is a box-dependent,  $\theta$ -independent and positive-definite quantity, and the extra-phase  $(M-1)\pi \delta_{i,N}$  follows from the anti-commuting rule for the fermion fields. We do not need the details in  $\Gamma_s$  here, which will be presented elsewhere. Recalling our lemma about the ‘charges’ of the shaded boxes, we can write the over-all product of these

sub-elements, namely, one of the elements in  $Z_M$ , as  $e^{i\phi} \prod_s \Gamma_s$  with the total phase  $\phi$  given by  $\phi = \sum_s n_s \theta + n(M-1)\pi = n[\varphi + (M-1)\pi]$ . Therefore, each element in  $\tilde{Z}_M$  (for allowed configurations) is positive-definite and  $\theta$ -independent. Consequently,

$$\frac{Z_M}{\tilde{Z}_M} = \sum_k P(k) e^{i n(k) [\varphi + (M-1)\pi]} = \sum_n P_n e^{i n [\varphi + (M-1)\pi]} \quad (5)$$

where  $P(k)$  is the ‘Boltzmann weight’ of a particular configuration (with a winding number  $n(k)$ ) in the auxiliary partition function  $\tilde{Z}_M$ , and  $P_n$  is a partial summation of the weights of all those configurations with a given winding number  $n$ . It should be pointed out that equation (5) is a topological consequence of the form of the Hamiltonian in equation (1), irrespective of the randomness in the lattice site energy  $\epsilon_i$ . A closer inspection reveals that equation (5) is also true even if there is randomness in the hopping matrix element  $t$  and the local phase  $\theta$  (so long as the total phase  $\varphi$  remains unchanged). Since  $P_n$  is independent of  $\varphi$ , the above equation serves in a unique way as an independent verification of the well-known conclusions that all equilibrium magnetic-field-dependent physics in the ring should be periodic in  $\Phi$  with a period  $\Phi_0$ , and that the relevant physical quantities for even and odd number of electrons are offset in  $\Phi$  by  $\Phi_0/2$  [6, 7].

Interestingly, if we ignore the anti-commutating rule of the fermion fields (e.g., in the case of a hard-core Bose system), equation (5) will be replaced by  $Z_M/\tilde{Z}_M = \sum_n P_n e^{i n \varphi}$ , which resembles the counterpart for a one-dimensional Bose system addressed by Pollock *et al* (see [14], equation (20)), who were able to evaluate the superfluid density from the winding number distribution. However, the important point in the present case lies in the Pauli interaction inherent in the Fermi statistics. In addition, equation (5) can also be obtained, in principle, by performing a gauge transformation [15]. The derivation presented here seems more straightforward.

Let us now consider the thermo-equilibrium persistent current pertaining to the mesoscopic ring,  $\langle J \rangle$ , where the current density operator  $J$  is given by

$$J = -\frac{ie t}{N\hbar} \sum_i (e^{i\theta} C_i^\dagger C_{i+1} - e^{-i\theta} C_{i+1}^\dagger C_i) \quad (6)$$

where  $-e$  is the electron charge. Conventionally, one would have to do simulations for the current–phase relation point-by-point in the phase  $\varphi$ . Furthermore, since the configurations with  $n = 0$  never contribute in average to the current, although they make major contributions to the average internal energy [12], a naive implementation of the HSS algorithm by keeping only the  $n = 0$  configurations would fail to give the correct current–phase relation. To get around this problem, it is essential to consider configurations with  $n \neq 0$ . These facts motivate us to consider the following way to perform an average for the current.

The first step in our approach is to write the average current as

$$\langle J \rangle = \frac{ek_B T}{\hbar} \frac{\partial}{\partial \varphi} \ln Z_M = \frac{ek_B T}{\hbar} \frac{\partial}{\partial \varphi} \ln \frac{Z_M}{\tilde{Z}_M} \quad (7)$$

where  $-k_B T \ln Z_M = F$  is the free energy of the canonical ensemble. The second equality reflects the fact that  $\tilde{Z}_M$  is independent of  $\theta$  (or  $\varphi$ ). The second step is to devise a Monte Carlo procedure that enables an importance sampling of all allowed configurations with different winding numbers. This can be achieved in a manner similar to that described in [12]. Consider the following free-boundary auxiliary partition function (also with  $M$  fermions)

$$\mathcal{Z}_M = \sum | \langle i_1 | U_1 | i_2 \rangle \langle i_2 | U_2 | i_3 \rangle \cdots \langle i_{2L} | U_{2L} | i_1 \rangle | \quad (8)$$

where the ends of the world-lines (at the time slices  $i_1$  and  $i_1'$ ) are now allowed to move horizontally across the shaded box when there is only one fermion in that box. In this way, new configurations with different winding numbers can be obtained. The Monte Carlo sweeps are done with respect to  $\mathcal{Z}_M$ , and whenever the states  $|i_1\rangle$  and  $|i_1'\rangle$  coincide, the configuration is sampled out. The expense of this technique is the running time for the intermediate configurations. All averages are done with respect to those *sampled configurations*. The probability that a particular configuration is sampled in a sequence of sampled configurations is exactly proportional to the corresponding ‘Boltzmann weight’ in  $\tilde{\mathcal{Z}}_M$  (rather than  $\mathcal{Z}_M$ ). In particular,  $P_n$  is simply the relative population of the configurations with a winding number  $n$ .

Furthermore, due to the time reversal symmetry built into  $\tilde{\mathcal{Z}}_M$  and  $\mathcal{Z}_M$ , theoretically one always has  $P_n = P_{-n}$  in the case of a homogeneous system. This is also true in the case of a random system since the world-lines self-average over the checkerboard in view of statistics. Thus equations (5) and (7) give

$$\langle J \rangle = \frac{ek_B T}{\hbar} \frac{\partial}{\partial \varphi} \ln \sum_n P_n \cos\{n[\varphi + (M-1)\pi]\} \quad (9)$$

which is the essential ingredient in our approach. Clearly, the advantage of the present algorithm lies in the fact that the global current–phase relation can be obtained once the  $\varphi$ -independent  $P_n$  are obtained, in contrast to the usual algorithm where the current–phase characteristics would have to be simulated point-by-point in  $\varphi$ . In addition, since only the population of the winding numbers need to be monitored in the simulation, the procedure is extremely simple. Finally, since the current is not evaluated from two independent averages, as would be the case if the previous Monte Carlo algorithms are naively implemented in the present case, the accuracy of the present algorithm is expected to be better. The computation time in each Monte Carlo sweep scales linearly with the area of the checkerboard (i.e., the number of the spatial sites times the number of the Trotter sites) [12].

For brevity, we define  $I = \langle J \rangle$  and  $f = \varphi/2\pi$  hereafter. The solid lines in the main panel of figure 2 are our Monte Carlo simulation results of the current–phase characteristics at a temperature  $T = t/8k_B$  for a 4-site ring with  $M = 2$  electrons ( $\epsilon_i = 0$ ) at various interaction strengths (only the cases  $V = 0, 2t, 4t$  are selected). The dashed line in the main panel shows the corresponding theoretical results at  $V = 0$  for this canonical ensemble<sup>†</sup>. Finite size effects (due to finite  $L$ ) in the simulations are minimal provided that  $L \geq 2N$  and  $\Delta\tau t \leq 0.5$ . The good agreement between our simulation result and the exact analytical result for  $V = 0$  in figure 2 lend support for our method. The top-left inset in figure 2 shows the population distribution  $P_n$  of the winding number  $n$  at  $V = 0$ , which is similar to a Gaussian distribution. The bottom-right inset in figure 2 shows more complete results for the interaction dependence of the maximum persistent current at the given temperature. One can see that the persistent current is suppressed more prominently at relatively stronger interactions ( $V \geq 2t$ ). In fact, in the thermodynamic limit  $N \rightarrow \infty$ , the half-filled spinless Hubbard model exhibits a zero-temperature phase transition from the normal liquid phase at  $0 \leq V \leq 2t$  to the Mott insulator phase at  $V > 2t$  [5]. The persistent current in the Mott phase vanishes. We shall return to this point later (see figure 4). Figures 3(a) and (b) show the current–phase characteristics at a sequence of temperatures in a 20-site ring with  $M = 12$  free and interacting electrons, respectively, where  $\Delta\tau t = 0.16$  in the simulations. Figure 3(c) shows the persistent current (with errors of the symbol size) at  $f = 0.25$  versus temperature, from which a quasi-exponential decay beyond a cross-over

<sup>†</sup> In the case of free fermions, the canonical ensemble partition function  $\text{Tr}_M e^{-\beta H}$  can be obtained with the diagonalized Hamiltonian in the Bloch state.

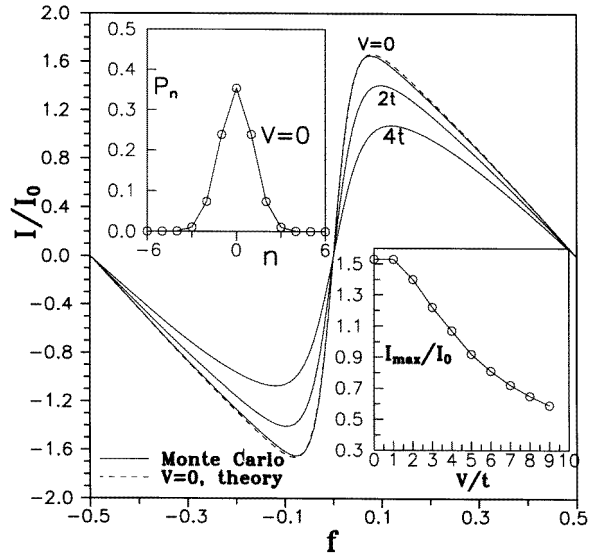


**Figure 2.** Current–phase characteristics for a 4-site ring with  $M = 2$  electrons at a temperature  $T = t/8k_B$  and at various interaction strengths. Here  $I_0 = et/4\hbar$ . The left inset shows the corresponding  $P_n$  versus  $n$  from the Monte Carlo simulations for  $V = 0$ . The right inset shows the interaction dependence of the maximum persistent current at the given temperature.

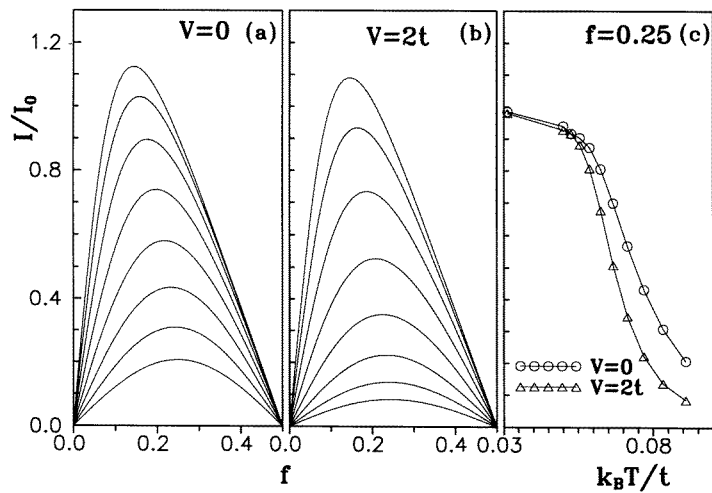


**Figure 3.** Current–phase characteristics for a 20-site ring with  $M = 12$  electrons ( $\epsilon_i = 0$ ). Here  $I_0 = et/20\hbar$ . (a)  $V = 0$ ,  $\beta t = 18, 17, \dots, 11$  for the curves with decreasing order in the amplitude. (b) The same as (a) except that  $V = 2t$ . (c) The current at  $f = 0.25$  versus the temperature.

temperature  $T^* \sim 0.05t/k_B$  is evident for each curve. At the low temperature side, the currents saturate to the zero-temperature limits. Note that the closer  $\varphi$  is to  $\varphi_m$ , where the free energy is a maximum, the lower the saturating temperature. Here  $\varphi_m = 2n\pi$  and  $(2n + 1)\pi$  for even and odd number of electrons, respectively. Although the system we

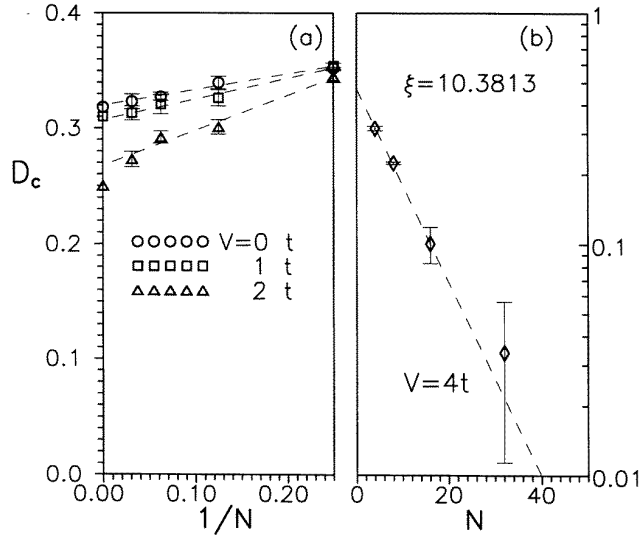


**Figure 4.** Size dependence of the zero-temperature-limit stiffness in the half-filled spinless model at various interaction strengths. (a)  $V/t = 0, 1, 2$ . The dashed lines are linear  $1/N$  extrapolation lines; (b)  $V = 4t$ . The dashed line represents exponential fitting.

are dealing with is a canonical ensemble, the above-mentioned behaviour is consistent with the picture in [3], although the system they considered was a *grand* canonical ensemble for *free* electrons. It is also clear from figure 3(c) that in this non-half-filled sector, the current is not suppressed by  $V$  in the zero-temperature limit. This is understandable because away from the half-filled sector, the nearest-neighbour interaction plays a progressively smaller role.

The so-called charge stiffness  $D_c$ , defined as

$$D_c = \frac{N}{2} \left. \frac{\partial^2 F}{\partial \varphi^2} \right|_{\varphi=\varphi_c}$$

where  $F$  is the free energy and  $\varphi_c$  is the value of  $\varphi$  at which  $F$  develops a minimum, can be obtained analytically for the spinless model in the thermodynamic limit at zero temperature in the half-filled sector [5]. From equation (5) it is also simply related to the above-mentioned winding number distribution as  $D_c = (N/2\beta) \sum_n n^2 P_n$ . The latter summation is nothing but the average square winding number. Notice that in the Bose system the stiffness corresponds to the superfluid density [14]. To compare our results with the analytical results [5], we have performed Monte Carlo simulations for various system sizes  $N$  and inverse temperatures. For the stiffness, we found no discrepancies between the results at  $\beta = N$  and  $\beta = 2N$  beyond the statistical error and thus take the results at this level of *low* temperatures as the zero-temperature limits. It deserves mentioning that exclusively in the half-filled sector, we do not need to open the checkerboard boundary at the Trotter direction to update the winding number. It is necessary to only include a global update procedure in the spatial direction whenever the occupation state in a time slice is a pure charge-density-wave-like state 10101010... This speeds up the simulations profoundly and enables us to simulate larger systems. The results for  $V/t = 0, 1, 2$  versus



the system size are plotted in figure 4(a). The symbols on the vertical axis are analytical results [5]. Evidently, as  $1/N \rightarrow 0$ , the extrapolated value from our Monte Carlo results agree excellently with the analytical results for  $V/t = 0, 1$ . The linear  $1/N$  extrapolation for  $V = 2t$  does not yield the rigorous result  $1/4$ . This can be clearly attributed to the following facts. On one hand, since  $V = 2t$  is the critical interaction for the liquid–Mott-insulator phase transition [5], the fluctuations in the system are strong and thus render a slightly poorer statistical accuracy. On the other hand a power-law instead of linear  $1/N$  extrapolation may be more appropriate. Figure 4(b) shows the size dependence of the zero temperature limit stiffness at  $V = 4t$ , from which we are able to extract the correlation length  $\xi = 10.38$  by fitting the stiffness as  $D_c \sim \exp(-N/\xi)$ . The fitted  $\xi$  is appealing compared with the analytical value  $\xi = 10.58$  at the same interaction strength [5].

Although we have only worked with the spinless Hamiltonian, the present algorithm can be easily generalized to a variety of more complex Hamiltonians, such as the coupled boson-fermion system and the system with spin-degrees of freedom included (in the absence of spin-flip interactions) addressed in [12]. The idea in this paper is also applicable to other topologically equivalent condensed matter systems, for example, the system with confined hard-core bosons considered in [16]. In addition, we have performed simulations for disordered rings with interacting spinless electrons and have found that both the interaction and the disorders suppress the amplitude of the persistent current. The details, with and without spin degrees of freedom for clean and disordered rings with general Coulomb interactions will be published elsewhere.

This work is supported by the RGC grant of Hong Kong under Grant No HKU262/95P and the National Center for Research and Development on Superconductivity of China.

## References

- [1] Hirsch J E 1987 *Quantum Monte Carlo Methods in Equilibrium and Non-equilibrium Systems* ed M Suzuki (Tokyo: Springer) p 205
- [2] Büttiker M, Imry Y and Landauer R 1983 *Phys. Lett. A* **96** 365  
Landauer R and Büttiker M 1985 *Phys. Rev. Lett.* **54** 2049
- [3] Cheung H F *et al* 1988 *Phys. Rev. B* **37** 6050
- [4] Schmid A 1991 *Phys. Rev. Lett.* **66** 80  
von Oppen F and Riedel E D 1991 *Phys. Rev. Lett.* **66** 84  
Altshuler B L, Gefen Y and Imry Y 1991 *Phys. Rev. Lett.* **66** 88
- [5] Shastry B S and Sutherland B 1990 *Phys. Rev. Lett.* **65** 243  
Sutherland B and Shastry B S 1990 *Phys. Rev. Lett.* **65** 1833
- [6] Zhu Jian-Xin and Wang Z D 1994 *J. Phys.: Condens. Matter* **6** L329  
Giamarchi T and Shastry B S 1995 *Phys. Rev. B* **51** 10915  
Roemer R A and Punnoose A *Phys. Rev. B* **52** 14809
- [7] Zhu Jian-Xin, Wang Z D and Li Sheng 1995 *Phys. Rev. B* **52** 14505
- [8] Lévy L *et al* 1990 *Phys. Rev. Lett.* **64** 2074  
Chandrasekhar V *et al* *Phys. Rev. Lett.* **67** 3578  
Mailly D, Chapelier C and Benoit A *Phys. Rev. Lett.* **70** 2020
- [9] Aharonov Y and Bohm D 1959 *Phys. Rev.* **115** 485
- [10] Abraham M and Berkovits R 1993 *Phys. Rev. Lett.* **70** 1509  
Bouzerar G, Poilbano D and Montambaux G 1994 *Phys. Rev. B* **49** 8258
- [11] Kato K and Yoshioka D 1994 *Phys. Rev. B* **50** 4943
- [12] Hirsch J E, Scalapino D J and Sugar R L 1981 *Phys. Rev. Lett.* **47** 1628  
Hirsch J E *et al* 1982 *Phys. Rev. B* **26** 5033
- [13] Suzuki M, Miyashita S and Kuroda A 1977 *Prog. Theor. Phys.* **58** 1377
- [14] Pollock E L and Ceperley D M 1987 *Phys. Rev. B* **36** 8343
- [15] Byers N and Yang C N 1961 *Phys. Rev. Lett.* **7** 46
- [16] Wang Z D and Zhu Jian-Xin 1995 *Phys. Rev. B* **52** 5275